Journal of Cardiovascular Disease Research
ISSN: 0975-3583, 0976-2833 VOL15, ISSUE 11, 2024

ALUMINIUM NANOPARTICLES TRIGGER SIZE-DEPENDENT PLATELET ACTIVATION: IMPLICATIONS FOR CARDIOVASCULAR RISK

Dr. Arijit Mazumdar

Assistant Professor, P A Sangma International Medical College and Hospital
Techno City, 9th Mile, Baridua, Ri Bhoi, Meghalaya, India

Abstract:

Endoprostheses are susceptible to tribological wear and biological processes that result in the release of particles, including aluminium nanoparticles (Al NPs), which can enter the bloodstream. The toxic effects of these nanoparticles on platelets have not been thoroughly investigated. This study aimed to assess the influence of Al NPs on human platelet function using an innovative quartz crystal microbalance with dissipation (QCM-D) approach, alongside various assays such as light transmission aggregometry, flow cytometry, optical microscopy, and transmission electron microscopy.

All tested Al NPs significantly increased both dissipation (D) and frequency (F), indicating platelet aggregation even at the lowest concentration of 0.5 µg/mL, with the exception of the largest Al NPs (80 nm). A size-dependent effect on platelet aggregation was noted for the 5–20 nm and 30–50 nm NPs, where larger particles resulted in smaller increases in D and F, but this was not observed for the 20–30 nm range. In conclusion, our findings demonstrate that smaller Al NPs (5–50 nm) induce platelet aggregation, while larger particles (80 nm) penetrate platelets, forming heterologous structures with them. Consequently, it is advisable for clinicians to monitor nanoparticle serum levels and platelet activation indices in patients with orthopaedic implants.

Keywords: **Aluminium nanoparticles, platelet aggregation, orthopaedic implants, toxicity, QCM-D.**

Introduction:

Total joint arthroplasty has emerged as one of the most effective treatment options in orthopaedic surgery, significantly enhancing patient mobility, alleviating pain, and improving overall quality of life. [4] Among these procedures, total hip arthroplasty (THA) and total knee arthroplasty (TKA) are the most common, with over one million THA surgeries performed globally each year and more than 100,000 and 700,000 TKA procedures conducted in the UK and the US, respectively.[1,2] These surgical interventions are primarily indicated for advanced osteoarthritis as well as for resections due to malignancies and haemophilic arthropathy.[3] Recently, there has been increasing interest in joint arthroplasty applications within neurosurgery, particularly total disc replacement (TDR), which is gaining traction as a viable alternative to cervical and lumbar fusion for degenerative disc disease. TDR preserves the functionality of intervertebral joints while offering favourable long-term outcomes. [5,6] To mitigate complications and reduce revision rates associated with THA, TKA, and TDR implants, various bearing materials have been developed. [9] While metal-on-polyethylene (MoP) bearings remain prevalent in hip and knee replacements, metal-on-metal (MoM) bearings have experienced a resurgence over the past two decades due to their lower dislocation risk . However, hip, knee, and intervertebral endoprostheses are susceptible to tribological wear and biological processes that release nanoparticles (NPs), metallo-organic complexes, inorganic oxides, and free ions into circulation. [11] These particles can accumulate in various organs, leading to local adverse effects such as cytotoxicity, genotoxicity, and damage to soft tissues. Ceramic prostheses are increasingly favoured due to their low wear rates and complication profiles. They are particularly desirable for younger and more active patients. Common ceramic bearings include ceramic-on-ceramic (CoC) and ceramic-on-polyethylene (CoP), with alumina (Al_2O_3) being a common component. Research indicates that ceramic implants containing Al_2O_3 can release alumina nanoparticles ranging from 5 to 90 nm in size. Most toxicological studies on implant-derived NPs have focused on cobalt and chromium materials, while emerging applications of Al_2O_3 NPs in nanomedicine have been explored. [12] However, investigations into the effects of NPs like Al NPs on blood components remain limited. Most studies have primarily examined their impact on lymphocytes, macrophages, and fibroblasts. [14,15] Given that aluminium nanoparticles are sufficiently small (<100 nm) to diffuse into the bloodstream, their potential effects on blood components warrant serious

consideration. Once in circulation, these nanoparticles may interact with platelets and potentially influence their aggregation properties. This interaction could heighten the risk of thrombotic or haemorrhagic events in patients with THA, TKA, or TDR implants—particularly crucial since these patients are already at increased risk for postoperative venous thromboembolism following TKA or THA procedures. [21] Despite this concern, the specific effects of Al NPs in circulation remain poorly understood. Previous research on other types of nanoparticles has indicated that their presence in the bloodstream can lead to widespread thrombosis. Given these considerations, it is imperative to address the safety of aluminium nanoparticles and their interactions with blood components such as platelets. [17] Therefore, our study aimed to investigate the impact of Al2O3 nanoparticles on platelet function using a novel quartz crystal microbalance with dissipation (QCM-D) methodology. [19] Traditional methods for measuring platelet aggregation may not adequately detect aggregation induced by nanoparticles at physiological concentrations; thus, a more sensitive approach is warranted. QCM-D was selected for this study due to its high sensitivity in detecting both platelet aggregation and microaggregation. [18,19] This technique allows for real-time monitoring of platelet microaggregates—precursors to larger thrombi—under conditions that mimic physiological flow dynamics and shear stress. In conclusion, understanding how aluminium nanoparticles affect platelet function is critical for assessing the safety of orthopaedic implants. The findings from our study will provide valuable insights into the potential risks associated with nanoparticle exposure in patients undergoing joint arthroplasty procedures.

Methods:

All the nanoparticles were sourced from nanografi company

Dispersion and Characterization of Nanoparticles

The aluminium oxide nanoparticles (Al_2O_3 NPs with 5 nm,10 nm,20nm,30nm, 80nm) utilized in this study were purchased from nanografi company These NPs were dispersed in phosphate-buffered saline (PBS) and platelet-poor plasma (PPP) at a concentration of 1 µg/mL. Size and zeta potential measurements were taken at 25 °C.

Blood Collection and Platelet Isolation

Peripheral blood samples were collected from healthy participants in tubes containing a 3.13% sodium citrate solution (in a 9:1 ratio) to prevent coagulation. Written informed consent was obtained from all participants, who abstained from medications or substances that could impact

platelet function for at least two weeks prior to the study. Platelet-rich plasma (PRP) and platelet-poor plasma (PPP) were prepared via centrifugation as previously described. PRP was diluted in PBS to reach a platelet concentration of 250,000/µL.

Platelet Aggregation Measured by Light Transmission Aggregometry

Platelet aggregation was assessed using a whole blood Lumi-aggregometer. NPs were sonicated in a water bath at 37 °C for 10 minutes. PRP samples were incubated with NPs at concentrations of 5, 10, and 25 µg/mL, and platelet aggregation was recorded for 10 minutes. Collagen (Chrono-log) at 5 µg/mL was used as a positive control, and platelet-poor plasma served as a reference blank. Data were calculated by measuring the percentage of maximal aggregation (with PPP transmission set at 100%).

Platelet Activation Monitored by Flow Cytometry

Flow cytometry was used to measure P-selectin expression in platelets exposed to NPs at 5 µg/mL. No stirring or vortexing was conducted to prevent premature platelet activation. Collagen-induced aggregation (5 µg/mL) served as the positive control, while resting platelets were used as a negative control. Once collagen-induced aggregation reached 50% maximal light transmission (as measured by Aggregometry), PRP samples with NPs were incubated in the dark at room temperature for 5 minutes with PAC-1 FITC antibodies (10 µg/mL). Samples were then diluted and analyzed within 5 minutes' cytometer. Platelets were identified based on forward- and side-scatter characteristics and fluorescence intensity was recorded for at least 30,000 events per sample. Data were analyzed using SPSS software with antibody binding expressed as the percentage of platelets positive for the antibody (collagen-induced platelets were set at 100%).

Platelet Aggregation Measured Using Quartz Crystal Microbalance with Dissipation

To study platelet aggregation under flow conditions, a quartz crystal microbalance with dissipation (QCM-D). Gold-coated quartz crystals were spin-coated with 0.5% w/v polystyrene and incubated with 100 µg/mL of fibrinogen (dissolved in PBS) for 1 hour. PRP samples were perfused at 37 °C at a rate of 100 µL/min using a peristaltic pump. NPs that induced platelet aggregation at 5 µg/mL in aggregometry or flow cytometry were analyzed using QCM-D. After NP sonication (10 minutes), platelet aggregation was monitored in real-time for 30 minutes using a software, recording frequency and dissipation changes. PPP served as the control.

Optical Microscopy

After QCM-D perfusion, crystals were examined under an Olympus BX43 optical microscope at 20x magnification. Photomicrographs were captured using an Olympus XM10 digital camera.

Statistical Analysis

Categorical data were analyzed using chi-squared tests. QCM-D results were expressed as frequency and dissipation shifts, analyzed using mixed ANOVAs. Independent t-tests were used for mean comparison, and a p-value < 0.05 was considered statistically significant.

Results:

Characterization of Aluminium Nanoparticles

The estimate, polydispersity list (PDI), and zeta potential of each aluminium nanoparticle (Al NP) were characterized utilizing a Zetasizer® Nano ZS, affirming the information given by the producer (Table 1).

Nanoparticles	**Zeta Size (SD), nm**		**Polydispersity Index (SD)**		**Zeta Potential, mV**	
	PPP	**DDH$_2$0**	**PPP**	**DDH$_2$0**	**PPP**	**DDH$_2$0**
Al_2O_3 5 nm	239	680 (83.3)	0.538	0.587 (0.069)	-	62.6
Al_2O_3 10 nm	42.8	93.1 (0.98)	0.320	0.219 (0.014)	-	46.0
Al_2O_3 20 nm	9.51	39.1 (0.74)	0.425	0.462 (0.052)	-	16.8
Al_2O_3 30 nm	43.9	89.8 (0.26)	0.447	0.245 (0.006)	-	47.7
Al_2O_3 50 nm	113	152 (1.01)	0.141	0.172 (0.027)	-	50.5
Al_2O_3 80 nm	614	1158 (156.00)	0.543	0.606 (0.132)	-	1.46

PPP: platelet-poor plasma, DDH20: double-distilled water

Table 1. Characteristics of included nanoparticles (Zetasizer).

Aluminium Nanoparticles Cause Platelet Aggregation:

Light transmission aggregometry (LTA) was utilized to degree platelet conglomeration, which was found to be concentration-dependent. Brooding of platelet-rich plasma (PRP) with Al NPs at concentrations of 25, 10, and 5 µg/mL affirmed platelet accumulation, whereas lower concentrations (Figure 1) appeared changed levels of accumulation. Platelets displayed the most considerable conglomeration in the nearness of collagen (positive control), whereas no conglomeration was watched with protein-poor plasma (PPP). Light transmission aggregometry comes about appearing concentration-dependent platelet accumulation. Collagen (5 µg/mL) was utilized as a positive control. The esteem of accumulation was given at 10 min of LTA appraisal. The impacts of Al NPs on platelet conglomeration were assist considered at lower concentrations utilizing quartz precious stone microbalance with dissemination (QCM-D). PRP perfusion of the sensor gems without modulators caused an discernible increment in dissemination (D) and a diminish in recurrence (F), with kept platelets affirmed by optical microscopy and transmission electron microscopy (TEM). Protein-poor plasma served as a control for kept proteins on the sensor gems. Noteworthy changes in F and D compared to controls were watched when sensor precious stones were perfused with PRP in the nearness of Al2O3 NPs (5, 10, 20, 30, 50, and 80 nm) at concentrations of 5, 2.5, 1, and 0.5 µg/mL. All Al NPs, but the biggest (80 nm), caused a noteworthy increment in D and F, showing platelet accumulation indeed at the most reduced concentration (0.5 µg/mL) (Figure 2).

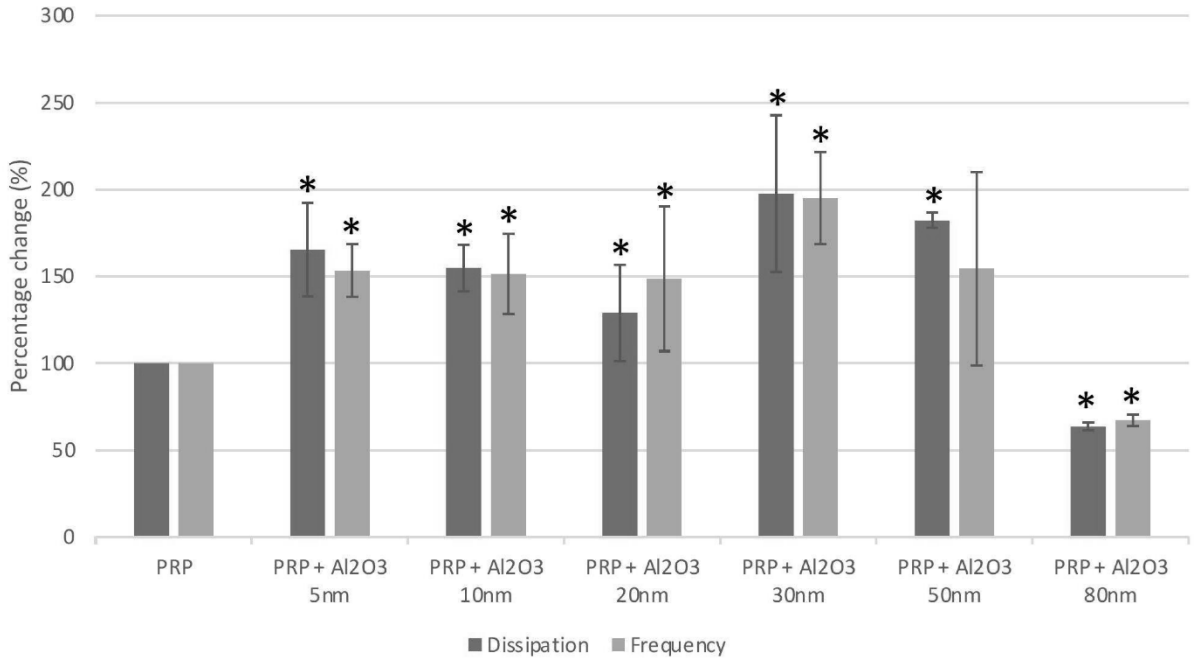

Figure 2. Impacts of aluminium nanoparticles (0.5 µg/mL) on platelet-rich plasma (PRP) utilizing quartz gem microbalancewith scattering. Information are communicated as cr uel ± standard deviation. * shows noteworthy contrast when compared to control (PRP).

The biggest increment in D happened with Al 30 nm NPs (197 ± 45.0).Effects of aluminium nanoparticles (0.5 µg/mL) on platelet-rich plasma (PRP) utilizing quartz gem microbalance with dissemination. Information are communicated as cruel ± standard deviation. * demonstrates critical distinction when compared to control (PRP).A size-dependent impact on platelet conglomeration was watched for the 5–20 nm and 30–50 nm NPs, with bigger Al NPs causing littler increments in D and F. In any case, this was not watched for the 20–30 nm NPs. Aluminium 80 nm NPs caused factually altogether littler changes in D and F compared to all other NP sizes.

Flow Cytometry Appears to produce no Platelet Enactment in the proximity of Al Nanoparticles

Flow cytometry was utilized to degree the impact of Al NPs (5, 10, 20, 30, 50, and 80 nm) at a concentration of 5 µg/mL on the level of platelet P-selectin expression.

No noteworthy increment in the number of P-selectin duplicates on the platelet surface was watched (Figure 3).

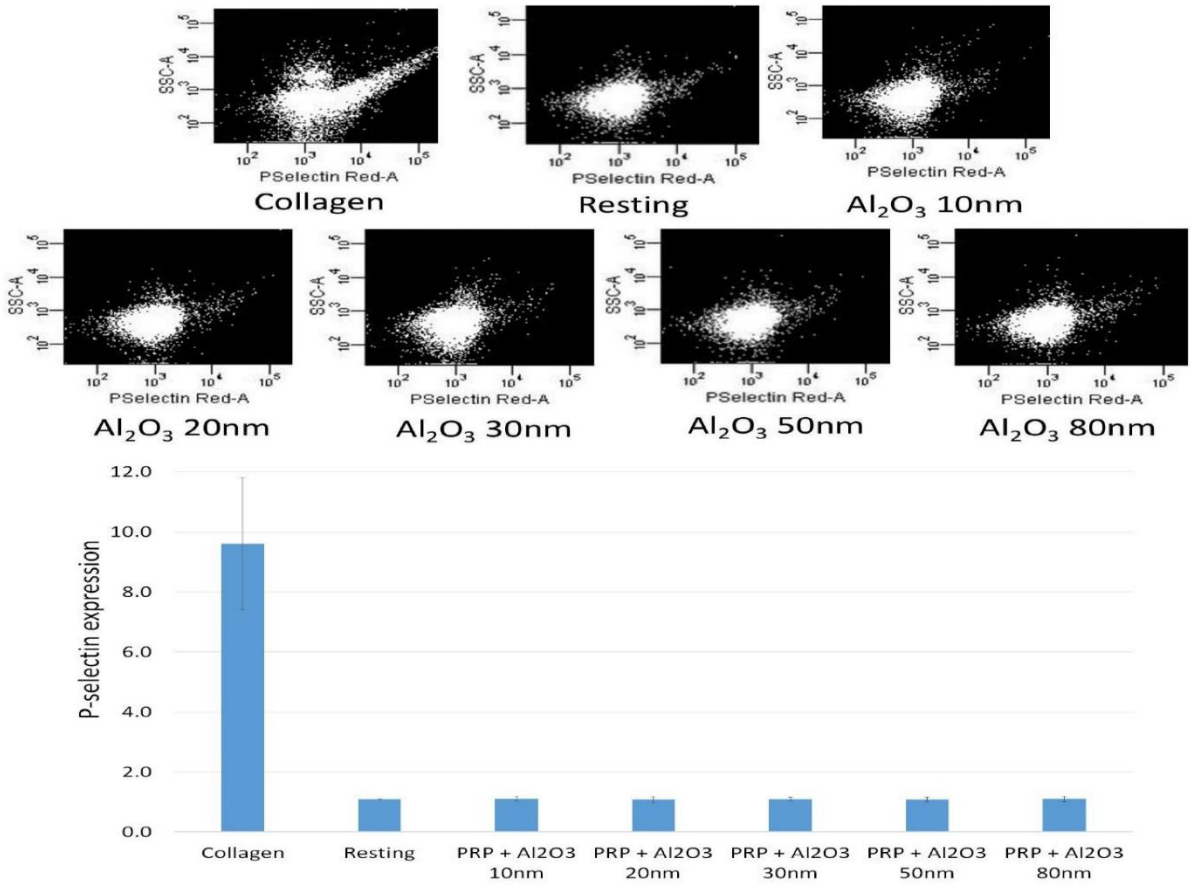

Figure 3. Stream cytometry comes about appearing investigations of P-selectin expression on platelets in the nearness of aluminium nanoparticles (5 µg/mL). Collagen (5 µg/mL)-induced accumulation was utilized as positive control and resting platelets were utilized as negative control.

Flow cytometry comes about appearing investigations of P-selectin expression on platelets in the nearness of aluminum nanoparticles (5 µg/mL). Collagen (5 µg/mL)-induced accumulation was utilized as a positive control, and resting platelets were utilized as a negative control.

<u>On Optical Microscopy there Appears Platelet coming together(Aggregating) on QCM-D Crystals</u>

Optical microscopy affirmed after experimentation that when PRP with aluminium nanoparticles are kept in an incubator at definite temperature in QCM-

D, uncovering expanded platelets comes together on the sensor surface which bears the crystalline unit (Figure 4)

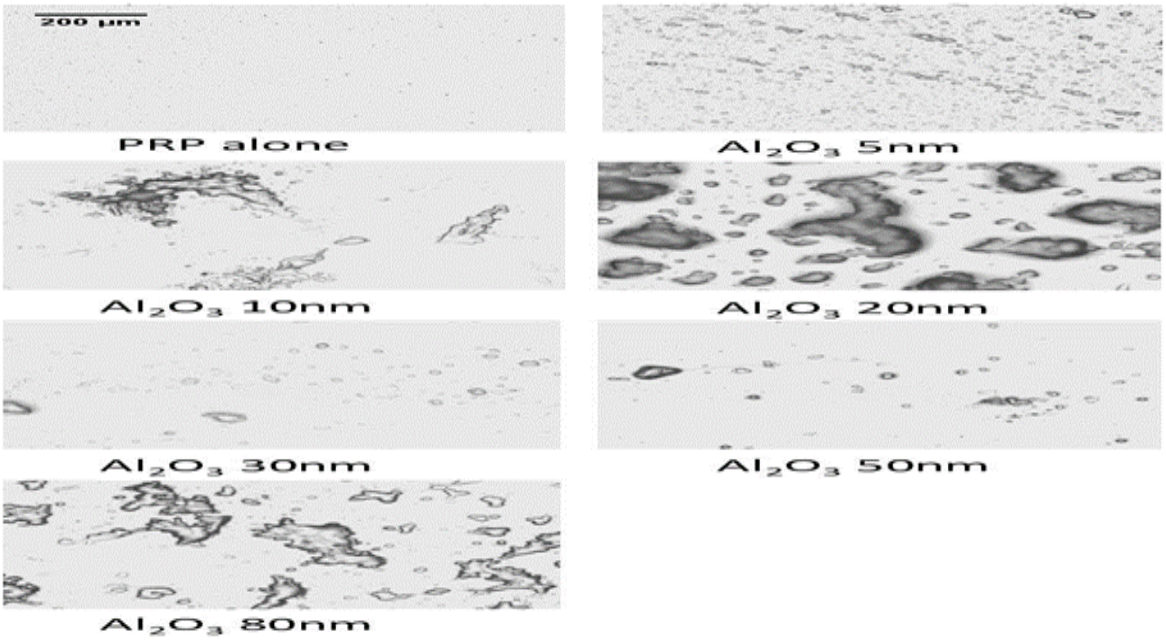

Figure 4. Micrographs of the surface of quartz gems as seen through optical microscopy. All light microscopy pictures are at 20× and at 0.5 ug/mL concentration.

Contrary to QCM-D, the biggest NPs (Al 80 nm) appeared collections of platelets that taken after totals. Micrographs of the surface of quartz gems as seen through optical microscopy. All light microscopy pictures are at 20× and at 0.5 µg/mL concentration. Transmission Electron Microscopy Appears Distinctive Components of Interaction with Platelets for Little (5–50 nm) and Huge (80 nm) Al Nanoparticles TEM examination of PRP tests hatched with Al NPs uncovered that Al2O3 5 nm–50 nm NPs driven to platelet enactment and accumulation (Figure5).

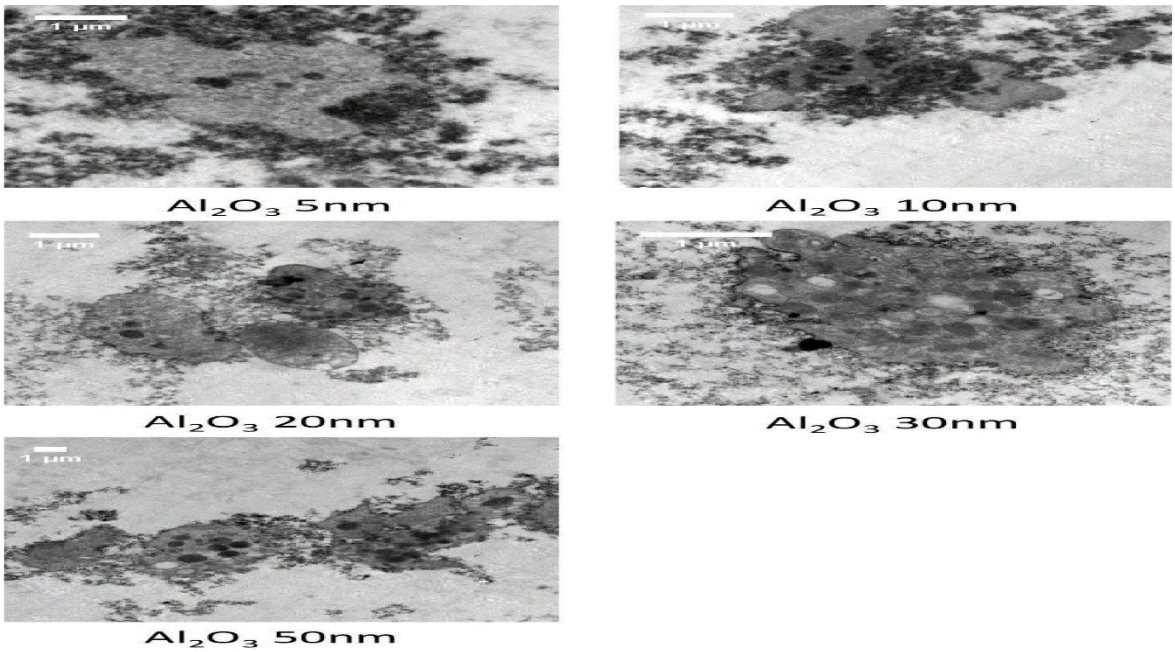

Figure 5. Transmission electron microscopy micrographs of the surface of sensor quartz precious stones taking after perfusion of platelet-rich plasma in the nearness of aluminium (5 nm–50 nm) nanoparticles (at a concentration of 0.5 µg/mL) appearing platelet actuation and conglomeration.

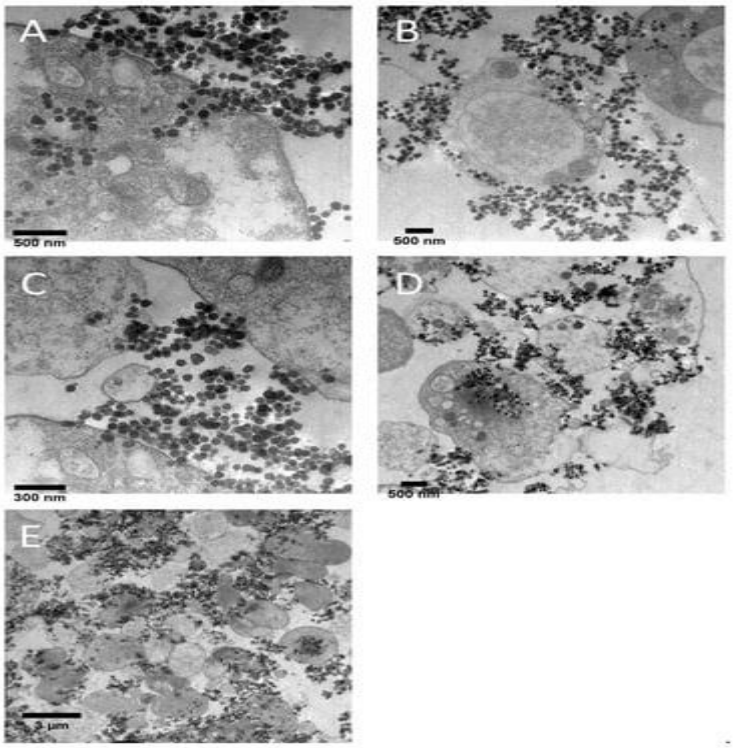

Figure 6. Transmission electron microscopy micrographs of the surface of sensor quartz precious stones appearing platelet section (A,B), bridging (C,D) and collections of a

few ineffectively enacted platelets taking after totals (E) taking after perfusion of platelet-rich plasma in the nearness of aluminium (80 nm) nanoparticles (at a concentration of 0.5 µg/mL).

The biggest Al NPs (80 nm) did not cause platelet accumulation but entered (Figure 6A,B) and bridged (Figure 6C,D) platelets, coming about in a few pitifully enacted platelets bridged by NPs, taking after totals (Figure 6E).Transmission electron microscopy micrographs of the surface of sensor quartz gems taking after perfusion of platelet-rich plasma in the nearness of aluminium (5 nm–50 nm) nanoparticles (at a concentration of 0.5 µg/mL) appearing platelet enactment and conglomeration. Transmission electron microscopy micrographs of the surface of sensor quartz gems appearing platelet passage (A,B), bridging (C,D), and collections of a few ineffectively actuated platelets taking after totals (E) taking after perfusion of platelet-rich plasma in the nearness of aluminium (80 nm) nanoparticles (at a concentration of 0.5 µg/mL.

Discussion:

This study aimed to examine the effects of aluminium nanoparticles (Al NPs) on platelet function, specifically focusing on their role in platelet activation and aggregation. Al NPs ranging from 5 to 80 nm were selected due to their prevalence in wear debris from ceramic-on-ceramic (CoC) and ceramic-on-polyethylene (CoP) joint replacements, which are increasingly favored over metal-on-metal (MoM) and metal-on-polyethylene (MoP) bearings due to their improved wear characteristics【21,22,38】. To assess the impact of Al NPs on platelet aggregation, we utilized quartz crystal microbalance with dissipation (QCM-D), a sensitive method that measures flow-induced platelet microaggregation【36,39,40,41】, and conducted subsequent microscopic analyses.

The results demonstrated that Al NPs influenced platelet function in a size-dependent manner. Al NPs between 5 nm and 50 nm in diameter induced platelet aggregation, whereas larger particles (80 nm) did not. Interestingly, while 80 nm Al NPs entered and bridged platelets, they did not activate them, instead forming quiescent aggregates resembling platelet clumps. This observation is particularly concerning given the known role of enhanced platelet activation in the pathophysiology of cardiovascular events【42】, suggesting that the presence of Al NPs in the bloodstream may contribute to such risks. Several studies have reported adverse cardiovascular effects caused by nanoparticles (NPs) in both in vitro and in vivo settings【

43,44,45】. This concern is heightened for individuals with pre-existing conditions such as diabetes, malignancies, or obstructive pulmonary disease, where increased platelet activation and hypercoagulability are commonly observed【46】. Moreover, Al NPs are frequently utilized in a variety of nanomedicine applications, including biosensors and drug delivery systems【26】, and have gained attention as potential bactericidal agents against multidrug-resistant bacteria【47】 due to their ability to disrupt bacterial membranes through reactive oxygen species production【27,28】.

Our QCM-D analysis confirmed that Al NPs, particularly those smaller than 80 nm, stimulated flow-dependent platelet microaggregation. This is consistent with previous studies that showed no impact of Al NPs (0.2 nm and 50 nm) on human fibroblasts【29,30】. However, prolonged exposure to Al NPs has been associated with cytotoxic effects, particularly for fibroblasts【48】. Interestingly, other research has shown that the cytotoxicity of Al NPs is dependent on their shape rather than size, as observed in macrophages【31】. This aligns with our findings, as Al NPs demonstrated cell-penetrating abilities, similar to observations with human fibroblasts [49]. These results highlight the importance of further investigation into the cellular entry mechanisms of Al NPs and their potential intracellular effects, particularly in circulating cell types such as platelets.

Increased serum metal ion levels have been reported in patients who have undergone total hip arthroplasty (THA), total knee arthroplasty (TKA), or total disc replacement (TDR), and these levels are linked to implant wear【50,51】. However, adverse tissue reactions have been observed even when metal ion levels are within normal ranges【52】. This discrepancy may be due to the limited number of studies analysing serum Al ion levels, particularly in patients with CoC implants【53,54,55】. In our study, QCM-D measurements revealed that Al NPs of different sizes produced varying levels of platelet aggregation, with the largest particles (80 nm) forming platelet aggregates without inducing significant activation. Transmission electron microscopy (TEM) confirmed these findings, showing that 80 nm Al NPs entered platelets but did not activate them, instead forming aggregate-like masses. Pairwise comparisons of platelet aggregation suggested a size-dependent effect, with smaller Al NPs (5–50 nm) causing greater aggregation【56】.

Nanoparticle-induced platelet activation is thought to occur via multiple mechanisms, including interactions with platelet surface receptors such as GPIIB/IIIa, which may lead to conformational changes and activation【58】. Additionally, NPs may bridge adjacent platelets, increasing aggregation【59】, or alter intracellular calcium levels, a key mediator of platelet function【60,61】. While our flow cytometry analysis did not show significant differences in P-selectin expression across NP sizes, the size-dependent effects observed in QCM-D suggest other mechanisms of platelet modulation by Al NPs in vivo.

Although this study simulated physiological conditions by examining NP-platelet interactions under flow, it did not account for interactions with red blood cells and endothelial cells, which are influenced by varying fluid shear stress【62】. Shear stress activates platelets via conformational changes in von Willebrand factor, facilitating its binding to platelet receptors【63】. Nanoparticles may further mediate this process, affecting blood rheology and viscosity【65】. Therefore, monitoring Al NP levels and platelet activation in patients undergoing joint replacement procedures may be critical, particularly in those with cardiovascular comorbidities【66】.

Conclusion:

In this study it is seen to explore the interactions between aluminium nanoparticles (Al NPs) and platelets using a novel quartz crystal microbalance with dissipation (QCM-D) methodology, which is capable of detecting microaggregation. Our findings revealed significant pro-aggregating effects of Al NPs on platelets, even at the lowest tested concentration of 0.5 μg/mL. Notably, smaller Al NPs (ranging from 5 to 50 nm) induced platelet aggregation, while larger Al NPs (80 nm) exhibited a bridging and penetrating effect, allowing them to enter platelets and form heterologous structures with them. Given these results, it is crucial to monitor aluminium nanoparticle levels and assess platelet function in patients with orthopaedic implants, as these interactions may pose risks for thrombotic events. This study highlights the importance of understanding how nanoparticles influence platelet behavior, which could have significant implications for patient safety and management in clinical settings.

Conflict of interest: There is no conflict of interest with any person or organisation.

References

1. Canovas, F.; Dagneaux, L. Quality of life after total knee arthroplasty. *Orthop. Traumatol. Surg. Res.* **2018**, *104*, S41–S46. [Google Scholar] [CrossRef] [PubMed]
2. Learmonth, I.D.; Young, C.; Rorabeck, C. The operation of the century: Total hip replacement. *Lancet* **2007**, *370*, 1508–1519. [Google Scholar] [CrossRef]
3. Patel, A.; Pavlou, G.; Mújica-Mota, R.E.; Toms, A.D. The epidemiology of revision total knee and hip arthroplasty in England and Wales: A comparative analysis with projections for the United States. a study using the national joint registry dataset. *Bone Jt. J.* **2015**, *97*, 1076–1081. [Google Scholar] [CrossRef] [PubMed] [Green Version]
4. Ferguson, R.J.; Palmer, A.J.; Taylor, A.; Porter, M.L.; Malchau, H.; Glyn-Jones, S. Hip replacement. *Lancet* **2018**, *392*, 1662–1671. [Google Scholar] [CrossRef]
5. Kremers, H.M.; Larson, D.R.; Crowson, C.S.; Kremers, W.K.; Washington, R.E.; Steiner, C.A.; Jiranek, W.A.; Berry, D.J. Prevalence of total hip and knee replacement in the United States. *J. Bone Jt. Surg. Am. Vol.* **2014**, *97*, 1386–1397. [Google Scholar] [CrossRef] [PubMed] [Green Version]
6. Wood, A.M.; Brock, T.M.; Heil, K.; Holmes, R.; Weusten, A. A Review on the Management of Hip and Knee Osteoarthritis. *Int. J. Chronic Dis.* **2013**, *2013*, 845015. [Google Scholar] [CrossRef] [Green Version]
7. Solimeno, L.P.; Pasta, G. Knee and Ankle Arthroplasty in Hemophilia. *J. Clin. Med.* **2017**, *6*, 107. [Google Scholar] [CrossRef] [Green Version]
8. Ament, J.D.; Yang, Z.; Nunley, P.; Stone, M.B.; Kim, K.D. Cost-effectiveness of cervical total disc replacement vs fusion for the treatment of 2-level symptomatic degenerative disc disease. *JAMA Surg.* **2014**, *149*, 1231–1239. [Google Scholar] [CrossRef] [Green Version]
9. Othman, Y.A.; Verma, R.; Qureshi, S.A. Artificial disc replacement in spine surgery. *Ann. Transl. Med.* **2019**, *7*, S170. [Google Scholar] [CrossRef]
10. Xia, Z.; Ricciardi, B.F.; Liu, Z.; von Ruhland, C.; Ward, M.; Lord, A.; Hughes, L.; Goldring, S.R.; Purdue, E.; Murray, D.; et al. Nano-analyses of wear particles from metal-on-metal and non-metal-on-metal dual modular neck hip arthroplasty. *Nanomed. Nanotechnol. Biol. Med.* **2017**, *13*, 1205–1217. [Google Scholar] [CrossRef]

11. Sands, D.; Schemitsch, E.H. The Role of Metal-on-Metal Bearings in Total Hip Arthroplasty and Hip Resurfacing. *HSS J.* **2017**, *13*, 2–6. [Google Scholar] [CrossRef] [Green Version]

12. Bozic, K.J.; Kurtz, S.; Lau, E.; Ong, K.; Chiu, V.; Vail, T.P.; Rubash, H.E.; Berry, D.J. The epidemiology of bearing surface usage in total hip arthroplasty in the United States. *J. Bone Jt. Surg. Ser. A* **2009**, *91*, 1614–1620. [Google Scholar] [CrossRef] [PubMed]

13. Matusiewicz, H. Potential release of in vivo trace metals from metallic medical implants in the human body: From ions to nanoparticles—A systematic analytical review. *Acta Biomater.* **2014**, *10*, 2379–2403. [Google Scholar] [CrossRef] [PubMed]

14. Papageorgiou, I.; Brown, C.; Schins, R.; Singh, S.; Newson, R.; Davis, S.; Fisher, J.; Ingham, E.; Case, C.P. The effect of nano- and micron-sized particles of cobalt-chromium alloy on human fibroblasts in vitro. *Biomaterials* **2007**, *28*, 2946–2958. [Google Scholar] [CrossRef]

15. Urban, R.M.; Jacobs, J.J.; Tomlinson, M.J.; Gavrilovic, J.; Black, J.; Peoc'h, M. Dissemination of wear particles to the liver, spleen, and abdominal lymph nodes of patients with hip or knee replacement. *J. Bone Jt. Surg. Ser. A* **2000**, *82*, 457–477. [Google Scholar] [CrossRef]

16. Drummond, J.; Tran, P.; Fary, C. Metal-on-Metal Hip Arthroplasty: A Review of Adverse Reactions and Patient Management. *J. Funct. Biomater.* **2015**, *6*, 486–499. [Google Scholar] [CrossRef] [Green Version]

17. Onega, T.; Baron, J.; MacKenzie, T. Cancer after total joint arthroplasty: A meta-analysis. *Cancer Epidemiol. Biomark. Prev.* **2006**, *15*, 1532–1537. [Google Scholar] [CrossRef] [Green Version]

18. Gill, H.S.; Grammatopoulos, G.; Adshead, S.; Tsialogiannis, E.; Tsiridis, E. Molecular and immune toxicity of CoCr nanoparticles in MoM hip arthroplasty. *Trends Mol. Med.* **2012**, *18*, 145–155. [Google Scholar] [CrossRef]

19. Jeffers, J.R.T.; Walter, W.L. Ceramic-on-ceramic bearings in hip arthroplasty: State of the art and the future. *J. Bone Jt. Surg. Ser. B* **2012**, *94*, 735–745. [Google Scholar] [CrossRef] [Green Version]

20. Hu, C.Y.; Yoon, T.R. Recent updates for biomaterials used in total hip arthroplasty. *Biomater. Res.* **2018**, *22*, 33. [Google Scholar] [CrossRef]

21. Zhang, Y.F.; Zheng, Y.F.; Qin, L. A comprehensive biological evaluation of ceramic nanoparticles as wear debris. *Nanomed. Nanotechnol. Biol. Med.* **2011**, *7*, 975–982. [Google Scholar] [CrossRef]

22. Wooley, P.H. How Has the Introduction of New Bearing Surfaces Altered the Biological Reactions to Byproducts of Wear and Modularity? *Clin. Orthop. Relat. Res.* **2014**, *472*, 3699–3708. [Google Scholar] [CrossRef] [Green Version]

23. Bijukumar, D.R.; Segu, A.; Souza, J.C.M.; Li, X.J.; Barba, M.; Mercuri, L.G.; Jacobs, J.J.; Mathew, M.T. Systemic and local toxicity of metal debris released from hip prostheses: A review of experimental approaches. *Nanomed. Nanotechnol. Biol. Med.* **2018**, *14*, 951–963. [Google Scholar] [CrossRef]

24. Behl, B.; Papageorgiou, I.; Brown, C.; Hall, R.; Tipper, J.L.; Fisher, J.; Ingham, E. Biological effects of cobalt-chromium nanoparticles and ions on dural fibroblasts and dural epithelial cells. *Biomaterials* **2013**, *34*, 3547–3558. [Google Scholar] [CrossRef] [Green Version]

25. Taterra, D.; Skinningsrud, B.; Pękala, P.A.; Tomaszewska, I.M.; Marycz, K.; Radomski, M.W.; Tomaszewski, K.A. In vitro effects of cobalt and chromium nanoparticles on human platelet function. *Nanotoxicology* **2021**, *15*, 52–65. [Google Scholar] [CrossRef]

26. Hassanpour, P.; Panahi, Y.; Ebrahimi-Kalan, A.; Akbarzadeh, A.; Davaran, S.; Nasibova, A.N.; Khalilov, R.; Kavetskyy, T. Biomedical applications of aluminium oxide nanoparticles. *Micro Nano Lett.* **2018**, *13*, 1227–1231. [Google Scholar] [CrossRef]

27. Wang, L.; Hu, C.; Shao, L. The antimicrobial activity of nanoparticles: Present situation and prospects for the future. *Int. J. Nanomed.* **2017**, *12*, 1227–1249. [Google Scholar] [CrossRef] [Green Version]

28. Ansari, M.A.; Khan, H.M.; Alzohairy, M.A.; Jalal, M.; Ali, S.G.; Pal, R.; Musarrat, J. Green synthesis of Al_2O_3 nanoparticles and their bactericidal potential against clinical isolates of multi-drug resistant Pseudomonas aeruginosa. *World J. Microbiol. Biotechnol.* **2015**, *31*, 153–164. [Google Scholar] [CrossRef]

29. Faye, P.A.; Roualdes, O.; Rossignol, F.; Hartmann, D.J.; Desmoulière, A. Engulfment of ceramic particles by fibroblasts does not alter cell behavior. *Biomed. Mater.* **2017**, *12*, 015023. [Google Scholar] [CrossRef]

30. Tsaousi, A.; Jones, E.; Case, C.P. The in vitro genotoxicity of orthopaedic ceramic (Al_2O_3) and metal (CoCr alloy) particles. *Mutat. Res. Genet. Toxicol. Environ. Mutagen.* **2010**, *697*, 1–9. [Google Scholar] [CrossRef]

31. Yamamoto, A.; Honma, R.; Sumita, M.; Hanawa, T. Cytotoxicity evaluation of ceramic particles of different sizes and shapes. *J. Biomed. Mater. Res. Part A* **2004**, *68*, 244–256. [Google Scholar] [CrossRef] [PubMed]

32. Catelas, I.; Petit, A.; Marchand, R.; Zukor, D.J.; Yahia, L.; Huk, O.L. Cytotoxicity and macrophage cytokine release induced by ceramic and polyethylene particles in vitro. *J. Bone Jt. Surg. Ser. B* **1999**, *81*, 516–521. [Google Scholar] [CrossRef]

33. Pedersen, A.B.; Mehnert, F.; Sorensen, H.T.; Emmeluth, C.; Overgaard, S.; Johnsen, S.P. The risk of venous thromboembolism, myocardial infarction, stroke, major bleeding and death in patients undergoing total hip and knee replacement: A 15-year retrospective cohort study of routine clinical practice. *Bone Joint J.* **2014**, *96*, 479–485. [Google Scholar] [CrossRef] [PubMed]

34. Radomski, A.; Jurasz, P.; Alonso-Escolano, D.; Drews, M.; Morandi, M.; Malinski, T.; Radomski, M.W. Nanoparticle-induced platelet aggregation and vascular thrombosis. *Br. J. Pharmacol.* **2005**, *146*, 882–893. [Google Scholar] [CrossRef] [PubMed] [Green Version]

35. Mills, N.L.; Törnqvist, H.; Gonzalez, M.C.; Vink, E.; Robinson, S.D.; Söderberg, S.; Boon, N.A.; Donaldson, K.; Sandström, T.; Blomberg, A.; et al. Ischemic and Thrombotic Effects of Dilute Diesel-Exhaust Inhalation in Men with Coronary Heart Disease. *N. Engl. J. Med.* **2007**, *357*, 1075–1082. [Google Scholar] [CrossRef] [Green Version]

36. Santos-Martinez, M.J.; Tomaszewski, K.A.; Medina, C.; Bazou, D.; Gilmer, J.F.; Radomski, M.W. Pharmacological characterization of nanoparticle-induced platelet microaggregation using quartz crystal microbalance with dissipation: Comparison with light aggregometry. *Int. J. Nanomed.* **2015**, *10*, 5107–5119. [Google Scholar] [CrossRef] [Green Version]

37. Larkin, C.M.; Breen, E.P.; Tomaszewski, K.A.; Eisele, S.; Radomski, M.W.; Ryan, T.A.; Santos-Martinez, M.-J. Platelet microaggregation in sepsis examined by quartz crystal microbalance with dissipation technology. *Platelets* **2018**, *29*, 301–304. [Google Scholar] [CrossRef]

38. Mochida, Y.; Boehler, M.; Salzer, M.; Bauer, T.W. Debris from failed ceramic-on-ceramic and ceramic-on-polyethylene hip prostheses. *Clin. Orthop. Relat. Res.* **2001**, *389*, 113–125. [Google Scholar] [CrossRef]

39. Santos-Martinez, M.J.; Inkielewicz-Stepniak, I.; Medina, C.; Rahme, K.; D'Arcy, D.M.; Fox, D.; Holmes, J.D.; Zhang, H.; Radomski, M.W. The use of quartz crystal microbalance with dissipation (QCM-D) for studying nanoparticle-induced platelet aggregation. *Int. J. Nanomed.* **2012**, *7*, 243–255. [Google Scholar] [CrossRef] [Green Version]

40. Tonda-Turo, C.; Carmagnola, I.; Ciardelli, G. Quartz crystal microbalance with dissipation monitoring: A powerful method to predict the in vivo behavior of bioengineered surfaces. *Front. Bioeng. Biotechnol.* **2018**, *6*, 158. [Google Scholar] [CrossRef]

41. Fatisson, J.; Azari, F.; Tufenkji, N. Real-time QCM-D monitoring of cellular responses to different cytomorphic agents. *Biosens. Bioelectron.* **2011**, *26*, 3207–3212. [Google Scholar] [CrossRef] [Green Version]

42. Badimon, L.; Padró, T.; Vilahur, G. Atherosclerosis, platelets and thrombosis in acute ischaemic heart disease. *Eur. Heart J. Acute Cardiovasc. Care* **2012**, *1*, 60–74. [Google Scholar] [CrossRef] [Green Version]

43. Abukabda, A.B.; Stapleton, P.A.; Nurkiewicz, T.R. Metal Nanomaterial Toxicity Variations within the Vascular System. *Curr. Environ. Health Rep.* **2016**, *3*, 379–391. [Google Scholar] [CrossRef] [Green Version]

44. Feng, Q.; Liu, Y.; Huang, J.; Chen, K.; Huang, J.; Xiao, K. Uptake, distribution, clearance, and toxicity of iron oxide nanoparticles with different sizes and coatings. *Sci. Rep.* **2018**, *8*, 2082. [Google Scholar] [CrossRef] [PubMed] [Green Version]

45. Cao, Y.; Gong, Y.; Liao, W.; Luo, Y.; Wu, C.; Wang, M.; Yang, Q. A review of cardiovascular toxicity of TiO_2, ZnO and Ag nanoparticles (NPs). *BioMetals* **2018**, *31*, 457–476. [Google Scholar] [CrossRef] [PubMed]

46. Fröhlich, E. Action of Nanoparticles on Platelet Activation and Plasmatic Coagulation. *Curr. Med. Chem.* **2016**, *23*, 408–430. [Google Scholar] [CrossRef] [Green Version]

47. Baptista, P.V.; McCusker, M.P.; Carvalho, A.; Ferreira, D.A.; Mohan, N.M.; Martins, M.; Fernandes, A.R. Nano-strategies to fight multidrug resistant bacteria—"A Battle of the Titans". *Front. Microbiol.* **2018**, *9*, 1498. [Google Scholar] [CrossRef] [Green Version]

48. Germain, M.A.; Hatton, A.; Williams, S.; Matthews, J.B.; Stone, M.H.; Fisher, J.; Ingham, E. Comparison of the cytotoxicity of clinically relevant cobalt-chromium and alumina ceramic wear particles in vitro. *Biomaterials* **2003**, *24*, 469–479. [Google Scholar] [CrossRef] [PubMed]

49. Radziun, E.; Dudkiewicz Wilczyńska, J.; Ksiazek, I.; Nowak, K.; Anuszewska, E.L.; Kunicki, A.; Olszyna, A.; Zabkowski, T. Assessment of the cytotoxicity of aluminium oxide nanoparticles on selected mammalian cells. *Toxicol. Vitr.* **2011**, *25*, 1694–1700. [Google Scholar] [CrossRef] [PubMed]

50. Hannemann, F.; Hartmann, A.; Schmitt, J.; Lützner, J.; Seidler, A.; Campbell, P.; Delaunay, C.P.; Drexler, H.; Ettema, H.B.; García-Cimbrelo, E.; et al. European multidisciplinary consensus statement on the use and monitoring of metal-on-metal bearings for total hip replacement and hip resurfacing. *Orthop. Traumatol. Surg. Res.* **2013**, *99*, 263–271. [Google Scholar] [CrossRef] [PubMed]

51. Reito, A.; Berryman, F.; Young, S.; Pandit, H.G.; Lainiala, O.; Eskelinen, A.; McConnell, J.; Judge, A.; Matharu, G.S.; Murray, D.W. Blood Metal Ion Thresholds to Identify Patients with Metal-on-Metal Hip Implants at Risk of Adverse Reactions to

Metal Debris. *J. Bone Jt. Surg.* **2017**, *99*, 1532–1539. [Google Scholar] [CrossRef] [Green Version]

52. Grammatopoulos, G.; Munemoto, M.; Pollalis, A.; Athanasou, N.A. Correlation of serum metal ion levels with pathological changes of ARMD in failed metal-on-metal-hip-resurfacing arthroplasties. *Arch. Orthop. Trauma Surg.* **2017**, *137*, 1129–1137. [Google Scholar] [CrossRef] [PubMed] [Green Version]
53. Weissinger, M.; Grübl, A.; Pöll, G. Serum-cobalt levels with metal-on-metal bearings in the cement-free total hip arthroplasty results covering two years; prospective study. *Acta Chir. Orthop. Traumatol. Cech.* **2011**, *78*, 410–415. [Google Scholar] [PubMed]
54. Savarino, L.; Padovani, G.; Ferretti, M.; Greco, M.; Cenni, E.; Perrone, G.; Greco, F.; Baldini, N.; Giunti, A. Serum ion levels after ceramic-on-ceramic and metal-on-metal total hip arthroplasty: 8-Year minimum follow-up. *J. Orthop. Res.* **2008**, *26*, 1569–1576. [Google Scholar] [CrossRef] [PubMed]
55. Grübl, A.; Weissinger, M.; Brodner, W.; Gleiss, A.; Giurea, A.; Gruber, M.; Pöll, G.; Meisinger, V.; Gottsauner-Wolf, F.; Kotz, R. Serum aluminium and cobalt levels after ceramic-on-ceramic and metal-on-metal total hip replacement. *J. Bone Jt. Surg. Ser. B* **2006**, *88*, 1003–1005. [Google Scholar] [CrossRef] [Green Version]
56. Montague, S.J.; Patel, P.; Martin, E.M.; Slater, A.; Quintanilla, L.G.; Perrella, G.; Kardeby, C.; Nagy, M.; Mezzano, D.; Mendes, P.M.; et al. Platelet activation by charged ligands and nanoparticles: Platelet glycoprotein receptors as pattern recognition receptors. *Platelets* **2021**, *32*, 1018–1030. [Google Scholar] [CrossRef]
57. Dwivedi, M.V.; Harishchandra, R.K.; Koshkina, O.; Maskos, M.; Galla, H.-J. Size Influences the Effect of Hydrophobic Nanoparticles on Lung Surfactant Model Systems. *Biophys. J.* **2014**, *106*, 289–298. [Google Scholar] [CrossRef] [Green Version]
58. Tomaszewski, K.A.; Radomski, M.W.; Santos-Martinez, M.J. Nanodiagnostics, nanopharmacology and nanotoxicology of platelet-vessel wall interactions. *Nanomedicine* **2015**, *10*, 1451–1475. [Google Scholar] [CrossRef]

59. Smyth, E.; Solomon, A.; Vydyanath, A.; Luther, P.K.; Pitchford, S.; Tetley, T.D.; Emerson, M. Induction and enhancement of platelet aggregation in vitro and in vivo by model polystyrene nanoparticles. *Nanotoxicology* **2015**, *9*, 356–364. [Google Scholar] [CrossRef]

60. Van Kruchten, R.; Braun, A.; Feijge, M.A.H.; Kuijpers, M.J.E.; Rivera-Galdos, R.; Kraft, P.; Stoll, G.; Kleinschnitz, C.; Bevers, E.M.; Nieswandt, B.; et al. Antithrombotic potential of blockers of store-operated calcium channels in platelets. *Arterioscler. Thromb. Vasc. Biol.* **2012**, *32*, 1717–1723. [Google Scholar] [CrossRef]

61. Jun, E.A.; Lim, K.M.; Kim, K.; Bae, O.N.; Noh, J.Y.; Chung, K.H.; Chung, J.H. Silver nanoparticles enhance thrombus formation through increased platelet aggregation and procoagulant activity. *Nanotoxicology* **2011**, *5*, 157–167. [Google Scholar] [CrossRef] [PubMed]

62. Saikia, J.; Mohammadpour, R.; Yazdimamaghani, M.; Northrup, H.; Hlady, V.; Ghandehari, H. Silica Nanoparticle–Endothelial Interaction: Uptake and Effect on Platelet Adhesion under Flow Conditions. *ACS Appl. Bio Mater.* **2018**, *1*, 1620–1627. [Google Scholar] [CrossRef] [PubMed]

63. Rana, A.; Westein, E.; Niego, B.; Hagemeyer, C.E. Shear-Dependent Platelet Aggregation: Mechanisms and Therapeutic Opportunities. *Front. Cardiovasc. Med.* **2019**, *6*, 141. [Google Scholar] [CrossRef]

64. Chen, Y.Y.; Syed, A.M.; MacMillan, P.; Rocheleau, J.V.; Chan, W.C.W. Flow Rate Affects Nanoparticle Uptake into Endothelial Cells. *Adv. Mater.* **2020**, *32*, 1906274. [Google Scholar] [CrossRef] [PubMed]

65. Michalczuk, U.; PRzekop, R.; Moskal, A. The effect of selected nanoparticles on rheological properties of human blood. *Bull. Polish Acad. Sci. Tech. Sci.* **2022**, *70*, e140437. [Google Scholar] [CrossRef]

66. Gomez-Garcia, M.J.; Doiron, A.L.; Steele, R.R.M.; Labouta, H.I.; Vafadar, B.; Shepherd, R.D.; Gates, I.D.; Cramb, D.T.; Childs, S.J.; Rinker, K.D. Nanoparticle localization in blood vessels: Dependence on fluid shear stress, flow disturbances, and flow-induced changes in endothelial physiology. *Nanoscale* **2018**, *10*, 15249–15261. [Google Scholar] [CrossRef] [PubMed]

67. Urban, R.M.; Tomlinson, M.J.; Hall, D.J.; Jacobs, J.J. Accumulation in liver and spleen of metal particles generated at nonbearing surfaces in hip arthroplasty. *J. Arthroplast.* **2004**, *19*, 94–101. [Google Scholar] [CrossRef]

68. Radomski, M.; Moncada, S. An improved method for washing of human platelets with prostacyclin. *Thromb. Res.* **1983**, *30*, 383–389. [Google Scholar] [CrossRef]

69. Shattil, S.J.; Cunningham, M.; Hoxie, J.A. Detection of activated platelets in whole blood using activation-dependent monoclonal antibodies and flow cytometry. *Blood* **1987**, *70*, 307–315. [Google Scholar] [CrossRef] [Green Version]

70. Sauerbrey, G. Verwendung von Schwingquarzen zur Wägung dünner Schichten und zur Mikrowägung. *Z. Für Phys.* **1959**, *155*, 206–222. [Google Scholar] [CrossRef]